PAPER

Fabrication and performance evaluation of a metal-based bimorph piezoelectric MEMS generator for vibration energy harvesting

To cite this article: Chun-Liang Kuo *et al* 2016 *Smart Mater. Struct.* **25** 105016

You may also like

- Piezoelectric micro energy harvesters based on stainless-steel substrates
  Shun-Chiu Lin and Wen-Jong Wu

- Piezoelectric MEMS generators fabricated with an aerosol deposition PZT thin film
  B S Lee, S C Lin, W J Wu et al.

- Fabrication of PZT MEMS energy harvester based on silicon and stainless-steel substrates utilizing an aerosol deposition method
  Shun-Chiu Lin and Wen-Jong Wu

Fabrication and performance evaluation of a metal-based bimorph piezoelectric MEMS generator for vibration energy harvesting

Chun-Liang Kuo[1], Shun-Chiu Lin[2] and Wen-Jong Wu[1]

[1] Department of Engineering Science & Ocean Engineering, National Taiwan University, Taipei, Taiwan
[2] Nano-Electro-Mechanical-Systems Research Center, National Taiwan University, Taipei, Taiwan

E-mail: wjwu@ntu.edu.tw

Abstract

This paper presents the development of a bimorph microelectromechanical system (MEMS) generator for vibration energy harvesting. The bimorph generator is in cantilever beam structure formed by laminating two lead zirconate titanate thick-film layers on both sides of a stainless steel substrate. Aiming to scavenge vibration energy efficiently from the environment and transform into useful electrical energy, the two piezoelectric layers on the device can be poled for serial and parallel connections to enhance the output voltage or output current respectively. In addition, a tungsten proof mass is bonded at the tip of the device to adjust the resonance frequency. The experimental result shows superior performance the generator. At the 0.5 g base excitation acceleration level, the devices pooled for serial connection and the device poled for parallel connection possess an open-circuit output voltage of 11.6 V_{P-P} and 20.1 V_{P-P}, respectively. The device poled for parallel connection reaches a maximum power output of 423 μW and an output voltage of 15.2 V_{P-P} at an excitation frequency of 143.4 Hz and an externally applied based excitation acceleration of 1.5 g, whereas the device poled serial connection achieves a maximum power output of 413 μW and an output voltage of 33.0 V_{P-P} at an excitation frequency of 140.8 Hz and an externally applied base excitation acceleration of 1.5 g. To demonstrate the feasibility of the MEMS generator for real applications, we finished the demonstration of a self-powered Bluetooth low energy wireless temperature sensor sending readings to a smartphone with only the power from the MEMS generator harvesting from vibration.

S Online supplementary data available from stacks.iop.org/SMS/25/105016/mmedia

Keywords: bimorph, piezoelectric, micro energy harvester, energy harvesting, lead zirconate titanate, PZT

(Some figures may appear in colour only in the online journal)

1. Introduction

In the past two decades, the applications of wireless sensors, like structural health monitoring, industrial process monitoring, and tire pressure monitoring and so on are getting more and more popular. The wireless sensors may have installed in rush environments or at remote locations [1], and thus such sensors are extremely difficult to replace and are expensive to maintain if the sensors are powered with batteries and batteries replacement is required. Despite that the power consumption of low-power radio circuit has been significantly improved in the past decade, the power consumption of such ultra-low-power wireless sensors is reduced to the scale of tens to hundreds of microwatts [2]. Therefore, the integrated sensor devices with embedded energy harvesters have become increasingly practical for generating power from ambient sources. Comparing the three possible ambient mechanical energy sources-piezoelectric, electromagnetic,
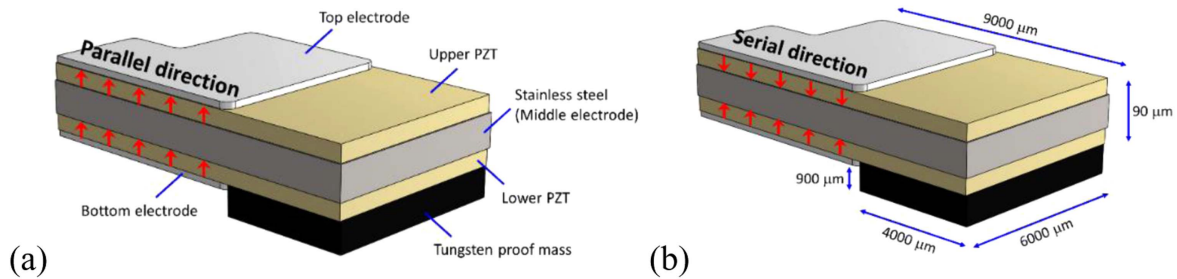
Figure 1. Schematic diagram of the bimorph piezoelectric MEMS generator: (a) device poled for parallel connection and (b) device pole for serial connection.

and electrostatic conversion [3], the energy produced from ambient vibrations of piezoelectric devices has higher density than that produced from electromagnetic or electrostatic devices [4]. Most piezoelectric energy harvesters involve using a cantilever-beam structure and incorporating micro-electromechanical system (MEMS) technology as the most effective fabrication technology for miniaturization [5]. Piezoelectric energy harvesters, in general, have bimorph and unimorph cantilever-beam structures [6], which generally entail using lead zirconate titanate (PZT) [7] and aluminum-nitride (AlN) [8] as piezoelectric materials. Although bimorph cantilever-beam structures considerably increase output voltage and power compared with unimorph cantilever-beam structures, they are manufactured on a micro scale because of the difficulty in fabricating piezoelectric material on the top and bottom of the cantilever beam. Thus, most micro piezoelectric energy harvesters have a unimorph structure [9].

Xu *et al* [10] successfully developed a bimorph generator with two piezoelectric PZT layers by using a screen-printing method. The energy harvester can have an approximately 33.2 μW power output at an excitation frequency of 346 Hz under 1.0 g acceleration vibration level test from both layers combined. Although the bimorph mode has been well developed for large-scale devices [4, 11–13], a bimorph piezoelectric device is difficult to fabricate for a micro-scale generator. In addition, none of the numerous PZT thick-film manufacturing processes can be used in bimorph piezoelectric MEMS generators.

This paper proposes the development of bimorph piezoelectric MEMS generators having PZT layers on both sides of a cantilever beam. Both PZT layers of the bimorph MEMS generator can be used to transform mechanical vibration energy into useful electrical power. Conventionally, PZT thin films are fabricated using a sol–gel process that is suitable for applying MEMS to fabricate 1–2 μm thin film. In this study, instead of using a conventional sol–gel process, PZT layers were deposited on the devices by using a home-made aerosol deposition machine that is suitable for depositing a PZT film of up to 3–50 μm thick. The PZT layers on both sides of the cantilever beam were fabricated using an aerosol deposition method [9].
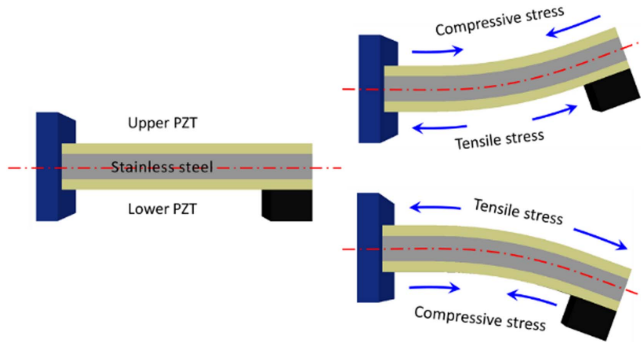
A metal-based bimorph piezoelectric MEMS generator with a cantilever-beam structure was constructed by laminating two PZT layers, an individual top electrode and a mutual bottom electrode. A proof mass was built at the tip of the beam for tuning the resonant frequency of the structure to match the most adaptable frequency that can be extracted from surrounding ambient vibrations. To obtain maximum stress and strain as well as to maximize the electric power output, the beam structure was designed to work at a resonant frequency for harvesting vibration energy from its surroundings. In this study, two poling configurations intended for parallel and serial connection were adopted for the upper and lower PZT layers of the bimorph piezoelectric MEMS generator [14]. The output performance and characteristics of the bimorph piezoelectric MEMS generator, such as power output, output voltage, and the impedance matching point for both poling directions, were evaluated.

Botterona *et al* [15] developed ultra-wideband (UWB) sensor node powered by a piezoelectric energy harvester, it demonstrates a tight integration of multiple technologies achieved thanks to the co-design of the harvesters, the UWB antenna and the electronics. The design is based on low-cost technologies, both for the harvesters and electronics. Kuo *et al* [16] shoed the initial design and evaluation of and demonstrate high output power, 423 μW was demonstrated when the bimorph energy harvester is in parallel configuration and drive at 1.5 g of base excitation. The design, the optimization and the characterization will be further detailed in this paper. Based on the energy harvester reported in this paper, a self-power Bluetooth low energy (BLE) wireless sensor is able to send temperature readings to a smart phone from a shaker simulating the base excitation level of motors or fans in heating, ventilation and air conditioning (HVAC) systems [17]. The details of this demonstration will also be presented in the last part of this paper.

2. Device design

Although the bimorph configuration of piezoelectric energy harvesters has been well developed in large-scale devices [4, 11–13], the fabrication of a micro-scale generator was still difficult. To increase the efficiency of the power output, a PZT layer is deposited on both sides of the stainless steel substrate of the bimorph piezoelectric MEMS generator. Figure 1 shows the schematic diagram of the bimorph piezoelectric MEMS generator in this study for harvesting low-frequency power targeting at 120 Hz to
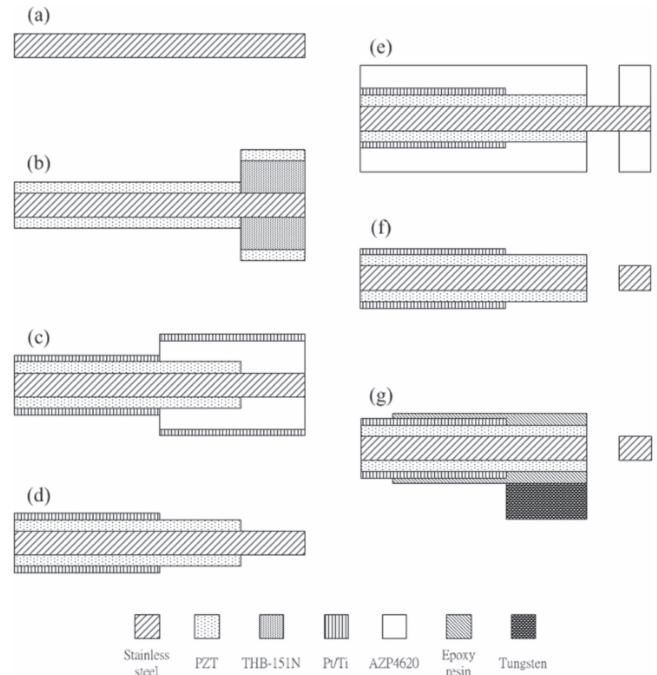
Figure 2. Schematic representation of the stress and strain distribution in a bimorph beam under bending.

Figure 3. Schematic diagram of the fabrication process based on a stainless steel substrate: (a) stainless steel substrate preparation, (b) upper and lower PZT deposition and patterning, (c) top and bottom electrode depositions, (d) lift-off by acetone, (e) beam shape etching and released beam, (f) PZT annealed at 650 °C, and (g) protective layer coating and bonding a proof mass.

harvest power from AC direct drive motors. The bimorph piezoelectric MEMS generator was primarily a micro-cantilever beam laminated with PZT layers on both sides and possessed a proof mass at the tip. The PZT layers on both sides could be poled in two directions: figure 1(a) shows the device poled for parallel connection, and figure 1(b) depicts the device poled for serial connection.

The bimorph piezoelectric MEMS generator in this study was designed as a $9000 \times 6000\,\mu m$ cantilever beam. The total thickness of this beam was $90\,\mu m$, formed by laminating two $15\,\mu m$ upper and lower PZT layers on a stainless steel substrate placed between thin electrodes at the top and bottom of the PZT layers. The lengths of the top and bottom electrodes were at a distance of $5000\,\mu m$ from the root; the width of the electrodes was $6000\,\mu m$. Stainless steel has excellent conductivity and thus can be used as a middle electrode between PZT layers. To adjust the resonant frequency of the bimorph piezoelectric MEMS generator, a proof mass having a length, width, and height of 4000, 6000, and $900\,\mu m$ respectively was installed at the bottom tip of the cantilever-beam structure. The built-in proof mass was easy to fabricate and thus could be used to tailor the resonance frequency of the generator to match the ambient vibrations. The deposited thicknesses of the upper and lower PZT layers were designed to be equal so that the stainless steel substrate was exactly at the neutral axis of the beam because of the symmetry. When the beam structure vibrated, the stress and strain levels of the beam were opposite to the PZT layers located on the two sides of the neutral axis. In other words, the upper and lower PZT layers underwent compression and extension individually; therefore, both layers utilized the d_{31} mode of the piezoelectric material to convert the external mechanical vibration energy into useful electrical energy. Figure 2 depicts this relationship in detail.

3. Fabrication process

The fabrication process of the bimorph piezoelectric MEMS generator is shown in figure 3. The device is fabricated on a $60\,\mu m$ stainless steel substrate, and the fabrication process is divided into seven steps. First, sulfuric acid (H_2SO_2) and hydrogen peroxide (H_2O_2) are used to clean the stainless steel

substrate. A $15\,\mu m$ lower PZT layer is then deposited and patterned using aerosol deposition method [9, 18, 19]. The deposition rate of the home-made aerosol PZT deposition machine was up to $0.1\,\mu m\,min^{-1}$. The PZT powder possessing particle sizes smaller than $1\,\mu m$ in diameter are placed into a container and shaken continuously to suspend the PZT powder. Either nitrogen or helium gas is introduced into the powder chamber to draw the PZT powder through the nozzle into the vacuumed deposition chamber. In the vacuum deposition chamber, the PZT powder is jetted out via the nozzle to bombard and coat the sample surface at a high speed. The upper PZT layer is then patterned using a lift-off process with a THB-151N negative photoresist and deposited for a $15\,\mu m$ thickness. The lower PZT layer is similarly patterned and deposited. After the PZT layer is deposited, the upper and lower electrodes are deposited with 30 nm Ti and 220 nm Pt by using an electron beam evaporator, followed by a patterned lift-off process. A wet etching process with aqua regia is then used to etch the stainless steel substrate from the back side until the beam is released. The PZT layers on the device is then annealed at 650 °C for 3 h in a furnace and then cooled to room temperature to obtain enhanced PZT characteristics. The cross-section view of the cantilever beam structure with two PZT layers, after the etching process, is shown in figure 4. The total thickness of the beam, including the upper PZT layer, stainless steel substrate, and lower PZT layer, is approximately $90\,\mu m$. An epoxy resin is then coated on to the surface of the device as a protective layer by using a soft scraper. Finally, the stainless steel substrate and tungsten
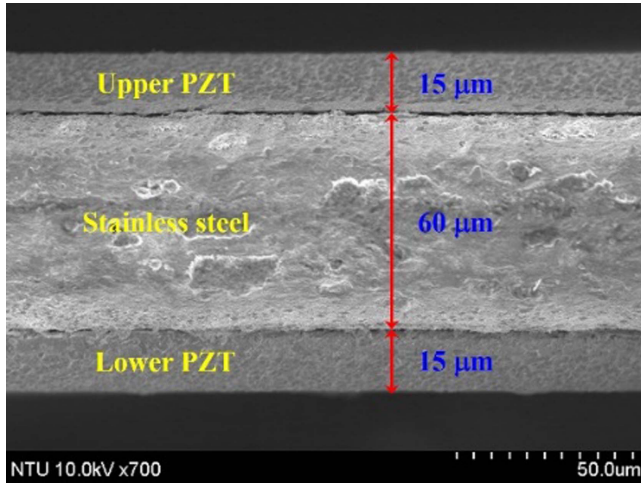
Figure 4. Scanned electron microscopy images of the cross-section of the beam and the double layer PZT.

proof mass is bonded with an epoxy glue. The finished cantilever beam composed of a double PZT layer with three laminated electrodes (with stainless steel as the middle electrode) and a proof mass at its tip is shown in figure 5. The fabrication of bimorph generators is processing on an area of 80×60 mm stainless steel plate substrate and 30 devices can be fabricated at the same time on single substrate. Three contact pads (top electrode, stainless steel substrate, and bottom electrode) of the image were used to measure the performance of the device. In addition, figure 5(b) shows that the size of the device is similar to the size of a paperclip.

4. Experimental setup and results

The experimental setup of measurement is shown in figure 6. The bimorph piezoelectric MEMS generator was placed on a shaker that provides a vibration source for the device. The shaker was driven by a sinusoidal signal from a function generator. The data acquisition device was DAQ-NI USB-6251 that had high input impedance (10 GΩ) and high sensitivity measurement accuracy, which can be assumed as an open circuit for measuring the output signal. The output signal of the device was connected to different load impedances for determining the relationship between the output characteristics and different load impedances. An accelerometer (B&K Type 4381) was placed with the bimorph piezoelectric MEMS generator to detect the given base excitation acceleration level.

In addition, the corresponding output average powers were calculated using the following equation:

$$P = \left(\frac{V_{p-p}}{2} \middle/ \sqrt{2} \right)^2 \middle/ R,$$

where V_{P-P} is the peak–peak value of the load output voltage, and R is the load resistance. The optimal load impedance for maximum power extraction was calculated by exciting the device either at the resonance or anti-resonance frequencies

[20–22]. In addition, the power output is measured at various load impedances [12].

4.1. PZT poling directions

The PZT layers were required being subjected to high electric field poling before the bimorph piezoelectric MEMS generator could be used. For the bimorph mode, two PZT layers can be poled in two different configurations, which can then be connected in parallel and serial. For the device poled parallel connection, the applied polling electric field is in the same direction for both the upper and lower PZT layers. The output voltage will be kept the same while the output current will be enhanced in this configuration. For the device poled for serial connection, the applied polling electric field is in opposite directions for the upper and lower PZT layers, and the output current will keep the same while the output voltage will be enhanced. During the poling process, the device was heated to 150 °C by using a hot plate, and a 15 V μm^{-1} externally applied electric field was applied for 60 min for each PZT layer. Finally, the device was gradually cooled at room temperature with the continuous application of an externally applied electric field.

For a bimorph piezoelectric MEMS generator, two PZT layers can be used separately or connected in a serial or parallel configuration. Figure 7(a) shows a device poled for parallel connection in which the top and bottom electrodes are connected to one port and the middle electrode is connected to the other port for the load, which is equivalent to a parallel circuit connection. Figure 7(b) shows a device poled for serial connection in which the load is connected to the top and bottom electrodes, which is equivalent to a serial circuit connection.
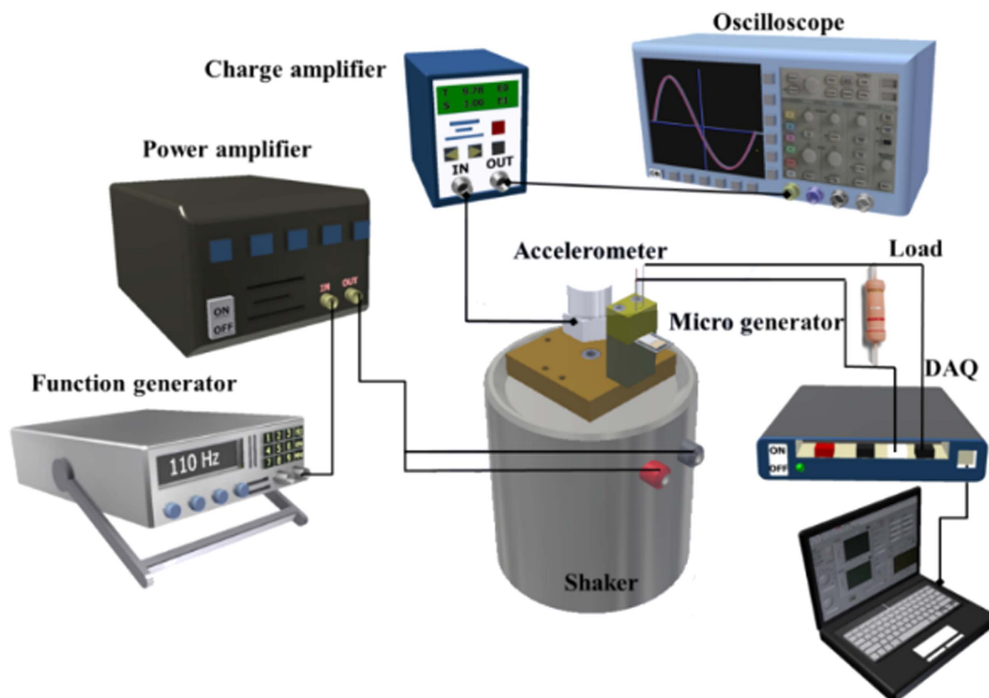
4.2. Device poled for parallel connection

Figure 8 shows the output voltage (peak-to-peak) and the power output at various loading impedances when excited at a resonant frequency with 0.5 g base excitation acceleration. The maximum peak-to-peak output voltage in open circuit condition was 11.6 V_{P-P} at the resonant frequency with 0.5 g base excitation acceleration. The output voltage decreased as the load impedance decreased. With 1.0 g base excitation acceleration, the power output achieved a peak value of 256 μW and an output voltage of 11.8 V_{P-P} when connected to an optimal load resistance, 68 kΩ.

In addition, the maximum power output was discovered when the bimorph device poled for parallel connection driven at 1.5 g base excitation acceleration. Figure 9 shows the relationship of the maximum power output and associated output voltage at various base excitation accelerations at optimal load impedance of 68 kΩ. Therefore, our device obtained a maximum power output and output voltage of 423 μW and 15.2 V_{P-P} under an impedance matching condition driven at 1.5 g base excitation acceleration.

4
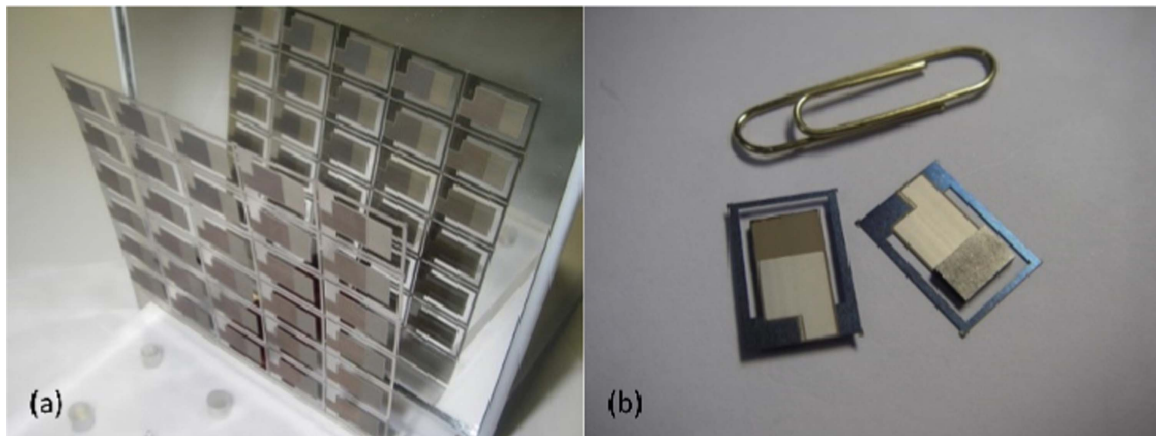
Figure 5. Photographs of (a) both sides of the bimo0rph mode based on stainless steel substrate and (b) the top and bottom view of the devices.

Figure 6. Experimental setup for measuring the piezoelectric MEMS generator.
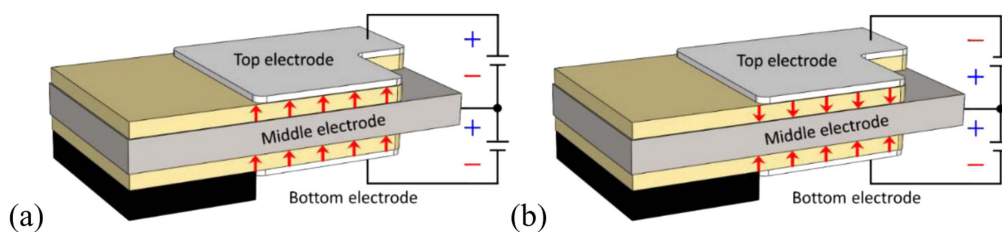

Figure 7. Load connection for a bimorph piezoelectric MEMS generator: (a) poled for parallel connection and (b) poled for serial connection.

4.3. Device poled for serial connection

Figure 10 shows the output voltage and power output at different load impedances when excited at 1.0 g base excitation acceleration. With 1.0 g base excitation acceleration,

the power output showed a peak value of 248 μW and a corresponding output voltage of 25.6 V_{P-P} when connected to a 330 kΩ optimal loading resistance.

The bimorph piezoelectric MEMS generator poled for serial connection was driven up to 1.5 g base excitation
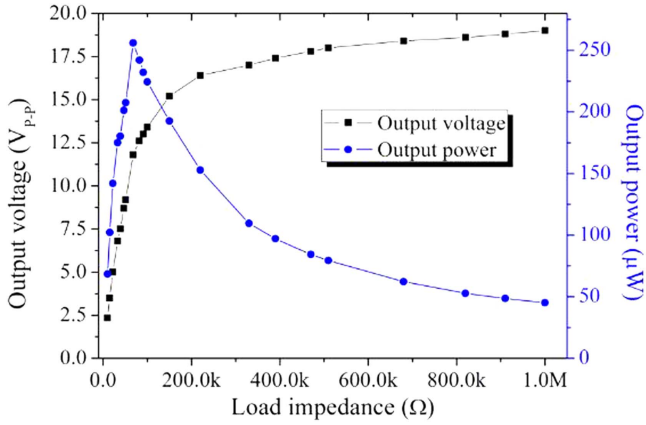
Figure 8. Output voltage and power output versus various load impedances excited at 1.0 g base excitation acceleration for the device poled for parallel connection.
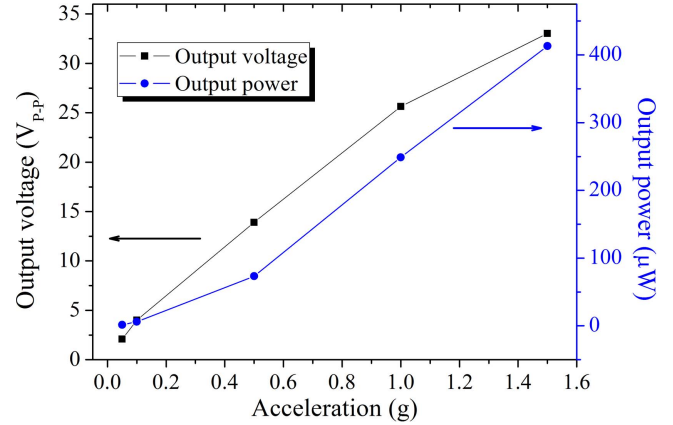
Figure 11. Relationship between maximum power output and associated output voltages at different based excitation accelerations at 330 kΩ optimal load impedance for a device poled for serial connection.

Figure 9. Relationship between maximum power output and corresponding output voltages at various applied base excitation accelerations at a 68 kΩ optimal load impedance for a device poled for parallel connection.
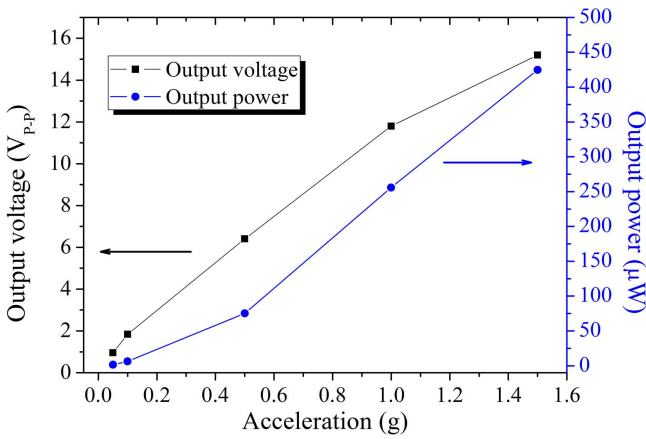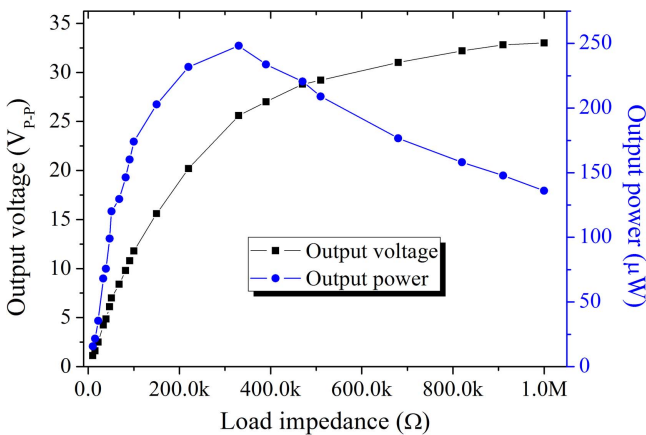

Figure 10. Output voltage and power output versus various load impedances when excited at 1.0 g base excitation acceleration for a device poled for serial connection.

acceleration connected with an optimal load impedance of 330 kΩ. Figure 11 shows the maximum power output and the corresponding output voltage at various base excitation accelerations. The device poled for serial connection achieved a maximum power output of 413 μW and an output voltage of 33.0 V_{P-P} under an impedance matching condition under 1.5 g base excitation acceleration.

Table 1 shows the summaries of the experimental results of the bimorph piezoelectric MEMS generator devices poled for serial and parallel connections. As shown, the optimal load of a device poled for serial connection was greater than that poled for parallel connection, because the optimal load is inversely proportional to the intrinsic static capacitance of the piezoelectric transducer [4]. The device poled for serial connection has the upper and lower PZT layers connected in series and thus have smaller total static capacitance corresponding to a greater optimal load resistance.

From table 1, we can see the performance, either the output power or voltage are not equal for the upper and lower layers for the bimorph generator. The upper layer always outperformed the lower layer. The major reason is the tungsten proof mass is relatively large and heavy compared with the cantilever beam body. The displacement of the beam is also large compared with the beam thickness and the tip displacement can be 3–5 mm for a 0.5 g base excitation which is considering to be a very large displacement relatively to a 60 μm beam body. When the generator is under base excitation, the displacement when bended down is much larger than the beam bended up because of the heavy proof mass. The maximum output power in a cycle is obtained when the beam is bended down to the lowest optimum point. When the beam is bended down with large displacement, the upper surface will stretch more than the lower surface and created larger strain on the top surface than the bottom surface. Because of the uneven displacement with longer half period bended down and the upper surface stretch more when the beam is bended down in large displacement, the voltage and

Table 1. Summary of the output performance of bimorph piezoelectric MEMS generators.

Polarization direction	Parallel	Series
Short-circuit f_{sc} (at 0.5 g)	143.4 Hz	140.8 Hz
Open-circuit f_{oc} (at 0.5 g)	143.5 Hz	140.9 Hz
Coupling coefficient k (at 0.5 g)	0.037	0.038
Output voltage under open circuit at 0.5 g (V_{p-p}) (upper layer/lower layer/both layer)	13.4/10.4/11.6	12.7/11.6/20.1
Damping coefficient ζ at 0.5 g	0.006	0.006
Quality factor Q at 0.5 g (both layer)	89.7	82.9
Capacitance C (nF) (upper layer/lower layer/both layer)	6.4/6.9/13.3	6.1/6.8/3.3
Load impedance at 1.5 g (kΩ) (upper layer/lower layer/both layer)	150/150/68	150/150/330
Max. power output at 1.5 g (μW) (upper layer/lower layer/both layer)	235/193/423	230/195/413
Max. voltage with load at 1.5 g (V_{p-p}) (upper layer/lower layer/both layer)	16.8/15.2/15.2	16.6/15.3/33.0

Table 2. Comparison of all published piezoelectric MEMS generators and our piezoelectric MEMS generators.

Author	Mode	A (g)	f (Hz)	Power (μW)	Area (mm^2)	Power density (μW mm^{-2})	Normalized energy density (μW g^{-1} Hz^{-1} cm^{-2})
Lee *et al* 2010 [23]	Bimorph	2.0	168	1.8	4.5	0.4	0.12
Yen *et al* 2011 [24]	3–1	1.0	853	0.17	0.245	0.69	0.08
Morimoto *et al* 2011 [25]	3–1	0.5	126	5.3	92.5	0.06	0.09
Aktakka *et al* 2011 [26]	3–1	1.5	154	205	49	4.2	1.81
Lei *et al* 2011 [27]	3–1	1.0	235	14	35.8	0.39	0.17
Defosseux *et al* [28]	3–1	0.25	214	0.62	5.6	0.11	0.21
Kanno *et al* 2012 [30]	3–1	1.0	1036	1.1	68	0.02	0.002
Tang *et al* 2012 [1]	3–1	1.0	514.1	11.5	2.5	4.6	0.89
Xu *et al* 2012 [10]	Bimorph	1.0	250	37.1	35.75	1.04	0.42
This paper (parallel)	Bimorph	1.5	143.5	423	54	7.8	3.6
This paper (series)	Bimorph	1.5	140.9	413	54	7.7	3.6

power output from the upper piezoelectric layer will always be higher than the lower piezoelectric layer for the bimorph piezoelectric generator.

Conversely, the device poled for parallel connection has the upper and lower PZT layers connected in parallel to the load resistance. Therefore, the device has four times the static capacitance compared with the device poled for serial connection, resulting in a different corresponding optimal load. Because of the polarization and load connection differences, the output voltage of the device poled for serial connection is approximately twice that of the device poled for parallel connection. Notably, even if a bimorph piezoelectric MEMS generator has different polarization directions with different output voltages and currents, the power output will be the same because the power density is identical and so is the effective total volume [4].

Table 2 presents a summary of the results of some published piezoelectric MEMS generators compared with the bimorph MEMS generators developed in this study. The device performance was evaluated with critical parameters

such as the cantilever-beam area, excitation frequency, generated power, power density, and normalized power density. The maximum area power densities and the normalized power densities of our bimorph piezoelectric MEMS generators were calculated to allow a fair comparison of the MEMS generators that operated at different accelerations and frequencies. Table 2 shows the superior performance of our device especially on the power density and normalized power density.

4.4. Demonstration of a self-powered wireless sensors

To prove the feasibility of field applications with the bimorph MEMS generator developed in this study, we setup a demonstration to power a wireless BLE temperature sensor with the MEMS generator harvesting power from vibration of a small shaker. The wireless sensor can than send temperature readings to a smartphone or a tablet computer. To finish the demonstration, we designed a package for the MEMS generator shown in figure 12(a). The demonstration package clamps the device as a cantilever beam and has a transparent

(a)

(b)
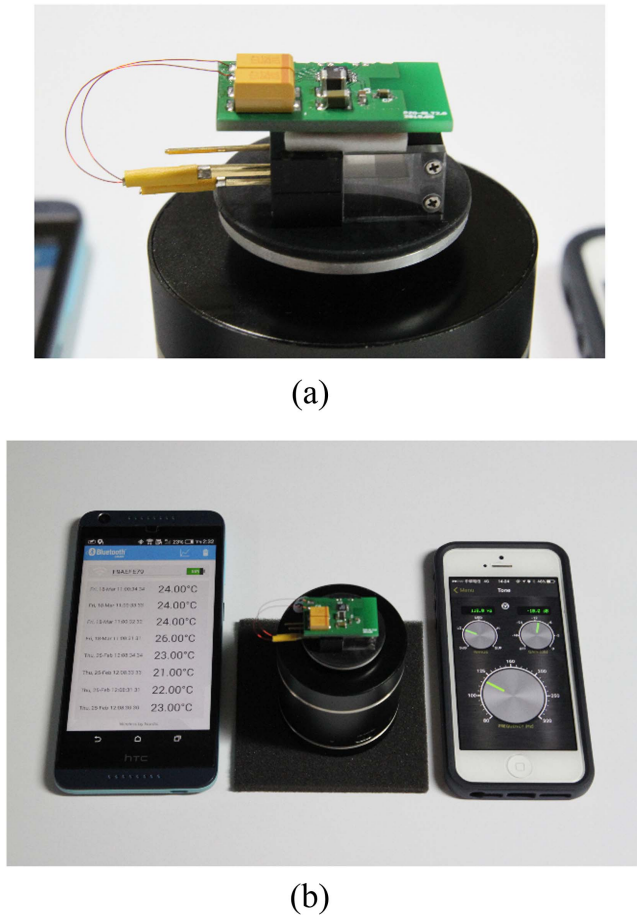
Figure 12. The experiment setup (a) the demonstration package clamping the MEMS generator and carrying a circuit board integrating the interfacing circuit and a BLE module (b) the complete demonstration setup.

side window, so the vibration of the cantilever beam can be seen when it is excited by external vibrations. The circuit carried on the demonstration package is a small circuit board integrating the interfacing circuit to the generator and the BLE module. The small shaker used in the demonstration is a Bluetooth resonant speaker which can be driven by Bluetooth connection ROM of a smartphone. The base excitation acceleration level of the small shaker is pre-calibrated with accelerometers and to simulate the vibration of 120 Hz and around 0.2 g acceleration closed to vibrations generated from the motors and fans in HVAC systems. Thanks to the advancement of low-power-radio-technology, the BLE module GW-STBT40 (Gwell Technology Co., Ltd, Taipei, Taiwan) based on lower-power BLE system-on-chip from Nordic semiconductor ASA (Oslo, Norway) has a peak power of 18.9 mW (1.8 V, 10.5 mA) when the wireless transmitter is turned on and transmitting in 0 dBM. The module also has an embedded solid state temperature sensor which will be used in this demonstration setup. Though the peak power requirement from the BLE module is higher that can be generated from the MEMS generator, in practical operations, the wireless sensor only need to send out readings periodically and the transmitting only last for a very short instance. It

is typical to have very small on-duty ratio compared with off-duty on operating the power consuming wireless transceiver. The interfacing circuit in between the BLE module and the MEMS generator includes a power conditioning circuit and an energy buffer, made with LTC-3588 integrated circuit from Linear Technology (Milpitas, CA, United States). LTC-3588 has a rectifier converting the AC power from the generator to DC form and then an internal DC–DC converter converting and regulating the output voltage to 1.8 V which is required by the BLE module. Two external 100 μF big capacitors are acted as an energy buffer and allowed duty ratio control that is matched with the real applications, which means the energy harvested from vibration can be collected into the buffer for a longer time and then deliver power to the external load with much higher instantaneous power. The complete setup is shown in figure 12(b). The small shaker was driven by a function generator app on the smartphone in the right-hand side through Bluetooth connection to simulate a vibration condition in HVAC systems. The temperature readings measured from the embedded temperature sensor inside the BLE module is then sent to the self-developed app modified from the example code from module vendor running on the smartphone in left-hand side.

The setup demonstrates a zero net energy self-power wireless temperature sensor to be powered only from power harvested from vibration. Figure 13(a) shows the oscilloscope waveform of supply voltage output from the power conditioning circuit to drive the BLE module. The energy buffer inside the power conditioning circuit can supply a steady voltage of 1.8 V, required of the BLE module for 27 s in a span of 46 s periodically with an on duty ratio of 58.7%. When the steady 1.8 V power is available to the BLE module, the embedded temperature sensor is powered and the reading is being sent to the smartphone with the wireless transmitter being turned on and the operation last smaller than 10 ms in the very beginning of the on period. The screenshot of the app receiving temperature readings from the self-powered wireless sensors is shown in figure 13(b).

5. Conclusions

This paper proposes a method for the metal-based fabrication and evaluation of a bimorph piezoelectric MEMS generator that can convert vibration energy into useful electrical energy from an ambient source. At the vibration frequency of the ambient source, we designed and fabricated a beam structure for adjusting the resonance frequency by varying the dimensions of the proof mass at the tip. The relationship between the output voltage and power output of the bimorph piezoelectric MEMS generator at different resistive loads was also investigated. The device poled for parallel connection has a maximum power output of 423 μW and an output voltage of 15.2 V$_\mathrm{P–P}$ driven at its resonant frequency and connected with optimal load. The device poled for serial connection has a maximum power output and output voltage of 413 μW and 33.0 V$_\mathrm{P–P}$ respectively when driven at its excitation frequency and connected with optimal load. The
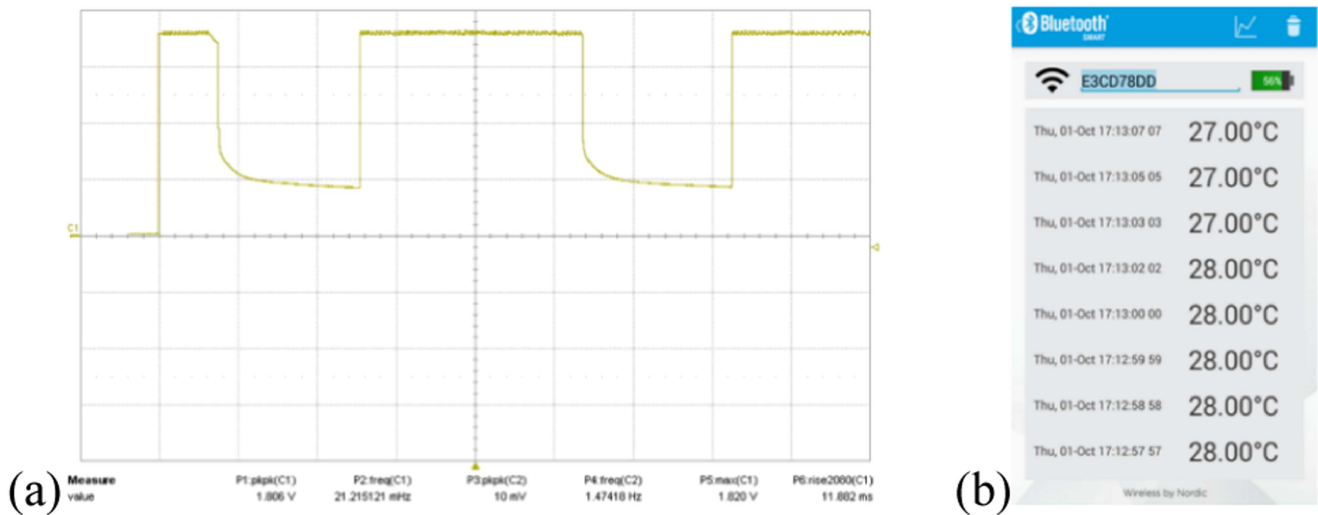
Figure 13. (a) Supply voltage waveform. (b) The screenshot of the app receiving temperature readings from the self-powered wireless sensors.

device poled for serial connection has a higher output voltage level than that poled for parallel connection. The device poled for parallel connection has a higher output current than that of the device poled for serial connection. The optimal load impedance of the device poled for serial connection (330 kΩ) is higher than that poled for parallel connection (68 kΩ). Compared with previous devices, the proposed device demonstrates superior power density and normalized power density performance. The device developed in this study is then used to power a battery-less wireless temperature sensor which can send temperature readings to a smartphone through BLE which proves the feasibility of real field application of the device.

Acknowledgments

References

[1] Rabaey J M, Ammer M J, da Silva J L, Patel D and Roundy S 2000 PicoRadio supports ad hoc ultra-low power wireless networking *Computer* **33** 42–8

[2] Amirtharajah R and Chandrakasan A P 1998 Self-powered signal processing using vibration-based power generation *IEEE J. Solid-State Circuits* **33** 687–95

[3] Roundy S, Leland E S, Baker J, Carleton E, Reilly E, Lai E, Otis B, Rabaey J M, Wright P K and Sundararajan V 2005 Improving power output for vibration-based energy scavengers *IEEE Pervasive Comput.* **4** 28–36

[4] Roundy S and Wright P K 2004 A piezoelectric vibration based generator for wireless electronics *Smart Mater. Struct.* **13** 1131–42

[5] Saadon S and Sidek O 2011 A review of vibration-based MEMS piezoelectric energy harvesters *Energy Convers. Manage.* **52** 500–4

[6] Renaud M, Karakaya K, Sterken T, Fiorini P, Van Hoof C and Puers R 2008 Fabrication, modelling and characterization of MEMS piezoelectric vibration harvesters *Sensors Actuators* A **145** 380–6

[7] Jeon Y B, Sood R, Jeong J H and Kim S G 2005 MEMS power generator with transverse mode thin film PZT *Sensors Actuators* A **122** 16–22

[8] Marzencki M, Ammar Y and Basrour S 2008 Integrated power harvesting system including a MEMS generator and a power management circuit *Sensors Actuators* A **145** 363–70

[9] Lin S C and Wu W J 2013 Piezoelectric micro energy harvesters based on stainless-steel substrates *Smart Mater. Struct.* **22** 045016

[10] Xu R, Lei A, Dahl-Petersen C, Hansen K, Guizzetti M, Birkelund K, Thomsen E V and Hansen O 2012 Screen printed PZT/PZT thick film bimorph MEMS cantilever device for vibration energy harvesting *Sensors Actuators* A **188** 383–8

[11] Lefeuvre E, Badel A, Richard C and Guyomar D 2005 Piezoelectric energy harvesting device optimization by synchronous electric charge extraction *J. Intel. Mat. Syst. Struct.* **16** 865–76

[12] Shu Y C and Lien I C 2006 Analysis of power output for piezoelectric energy harvesting systems *Smart Mater. Struct.* **15** 1499–512

[13] Shu Y C and Lien I C 2006 Efficiency of energy conversion for a piezoelectric power harvesting system *J. Micromech. Microeng.* **16** 2429–38

[14] Smits J G, Dalke S I and Cooney T K 1991 The constituent equations of piezoelectric bimorphs *Sensors Actuators* A **28** 41–61

[15] Botterona C *et al* 2013 A low-cost UWB sensor node powered by a piezoelectric harvester orsolar cells *Sensors Actuators* A **239** 127–36

[16] Kuo C L, Lin S C and Wu W J 2014 Fabrication and characteristic of piezoelectric bimorph MEMS generators based on stainless steel substrate for vibration generator *Int. Conf. on Adaptive Structures and Technologies (ICAST)*

[17] Hsieh Y C, Lin T K, Chen J J and Wu W J 2015 Self-powered wireless temperature sensor with piezoelectric energy

harvester fabricated with metal-mems process *Int. Conf. on Adaptive Structures and Technologies (ICAST)*

[18] Wang X Y, Lee C Y, Hu Y C, Shih W P, Lee C C, Huang J T and Chang P Z 2008 The fabrication of silicon-based PZT microstructures using an aerosol deposition method *J. Micromech. Microeng.* **18** 055034

[19] Lin S C and Wu W J 2013 Fabrication of PZT MEMS energy harvester based on silicon and stainless-steel substrates utilizing an aerosol deposition method *J. Micromech. Microeng.* **23** 125028

[20] DuToit N E and Wardle B L 2007 Experimental verification of models for microfabricated piezoelectric vibration energy harvesters *AIAA J.* **45** 1126–37

[21] Halvorsen E 2008 Energy harvesters driven by broadband random vibrations *J. Microelectromech. Syst.* **17** 1061–71

[22] Saggini S, Giro S, Ongaro F and Mattavelli P 2010 Implementation of reactive and resistive load matching for optimal energy harvesting from piezoelectric generators *2010 IEEE 12th Workshop on Control and Modeling for Power Electronics (COMPEL)* pp 1–6

[23] Lee B S, Lin S C and Wu W J 2010 Fabrication and evaluation of a mems piezoelectric bimorph generator for vibration energy harvesting *J. Mech.* **26** 493–9

[24] Yen T T, Hirasawa T, Wright P K, Pisano A P and Lin L W 2011 Corrugated aluminum nitride energy harvesters for high energy conversion effectiveness *J. Micromech. Microeng.* **21** 085037

[25] Morimoto K, Kanno I, Wasa K and Kotera H 2010 High-efficiency piezoelectric energy harvesters of *c*-axis-oriented epitaxial PZT films transferred onto stainless steel cantilevers *Sensors Actuators* A **163** 428–32

[26] Aktakka E E, Peterson R L and Najafi K 2011 Thinned-PZT on SOI process and design optimization for piezoelectric inertial energy harvesting *Transducer's 11 (Beijing, China)* pp 1649–52

[27] Lei A, Xu R, Thyssen A, Stoot A C, Christiansen T L, Hansen K, Lou-Moller R, Thomsen E V and Birkelund K 2011 MEMS-based thick film PZT vibrational energy harvester *2011 IEEE 24th Int. Conf. on Micro Electro Mechanical Systems (MEMS)* pp 125–8

[28] Defosseux M, Allain M, Defay E and Basrour S 2012 Highly efficient piezoelectric micro harvester for low level of acceleration fabricated with a CMOS compatible process *Sensors Actuators* A **188** 489–94

[29] Kanno I, Ichida T, Adachi K, Kotera H, Shibata K and Mishima T 2012 Power-generation performance of lead-free $(K, Na)NbO_3$ piezoelectric thin-film energy harvesters *Sensors Actuators* A **179** 132–6

[30] Tang G *et al* 2012 Fabrication and analysis of high-performance piezoelectric MEMS generators *J. Micromech. Microeng.* **22** 065017